Egyptian Journal of Petroleum 28 (2019) 383–392

HOSTED BY

Contents lists available at ScienceDirect

Egyptian Journal of Petroleum

journal homepage: www.sciencedirect.com

Full Length Article

Influences of uncertainty in well log petrophysics and fluid properties on well test interpretation: An application in West Al Qurna Oil Field, South Iraq

Ali Y. Jirjees [a], Abdulaziz M. Abdulaziz [b,*]

[a] Petroleum Engineering Department, College of Engineering, Kirkuk University, Kirkuk, Iraq
[b] Mining, Petroleum, and Metallurgical Engineering Department, Faculty of Engineering, Cairo University, Giza 12316, Egypt

ARTICLE INFO

Article history:
Received 25 February 2019
Revised 24 July 2019
Accepted 24 August 2019
Available online 13 September 2019

Keywords:
Uncertainty analysis
Well log petrophysics
Well test
West Al Qurna Oil Field
Iraq

ABSTRACT

In the present study, well log and well test data of 3 wells are investigated in details using Interactive Petrophysics (IP 3.5) software and KAPPA Workstation 2016 (Saphir) to examine the reservoir properties and to evaluate the effect of uncertainty in well logs interpretation on well test results. This involves the variations in the output value induced by random, systematic and model-based errors of the petrophysical input data. Results of well test uncertainty analysis indicated that the effective permeability calculations are strongly affected by the pay thickness uncertainty in Mishrif Formation with changes between 14.5% and 47%. Significant influences are related to pressure (∼10%), μo and Bo (∼9%), ?? (∼6%), and Sw (∼5%). Alternatively, radius of investigation calculations reported slight influences attributed to Sw (∼9%) and porosity (5%) uncertainties, with minimal influence by Bo, μo, and pressure. The skin factor calculations, however, showed a great sensitivity towards the pressure measurements up to 35%. Compared to fluid data, petrophysics uncertainty analysis showed marked influences on the effective permeability, skin factor and radius of investigation. These results show the importance of accurate reservoir petrophysics on well test interpretation that may change the calculated values between 10 and 50% that strongly influence the expected well performance.

1. Introduction

Optimum reservoir characterization and management mandate a faithful description to reservoir units [1] from different sources including well logs, core samples, well test, and production data [2–4]. Well test analysis became a valuable reservoir characterization tool to recognize heterogeneous reservoir behaviors such as double and composite permeability, partial penetration or limited entry, horizontal wells analysis, and the wide range of boundary effects [5]. Formation evaluation using well logs and core data interpretation typically targets certain rock properties that mostly affected by lithology and depositional environment [4]. In addition, petrophysical cutoffs may significantly affect reservoir characterization for both static and dynamic models that considerably influence the realizations of the asset value [6]. Several analytical and statistical methods are tested to quantify the overall uncertainty parameters and address the possible source of uncertainty in petrophysical analysis [7]. Model and systematic uncertainties have been identified as the chief sources of uncertainty in computations of hydrocarbon in place, and a holistic approach is recommended to ensure considering the proper range for uncertain petrophysical parameters [8].

Reservoir parameters uncertainty remains a challenge in reservoir management, but a reliable petrophysical analysis could encompass a limited number of skeptic reservoir properties [9]. To tackle this challenge, Monte Carlo simulation may help in analyzing the probable scenarios for such uncertain parameters using error analysis models [10]. It is first used in the business [11], and with the advent of the computer, mathematical models are created to simulate complex projects including petroleum industry [12,13]. Monte Carlo simulation helped understanding the risk in reserve estimation, and consequently economics, by quantifying various variables uncertainty using probability and possible values [14]. It could be a suitable method to quantify uncertainty, but only when an appropriate interpretation model is adopted [15,16]. Using stochastic approaches not only explain and justify final petrophysical uncertainty but also provide recommendations for new data acquisitions to diminish the overall uncertainty [17,18].

Peer review under responsibility of Egyptian Petroleum Research Institute.
* Corresponding author.
E-mail address: amabdul@miners.utep.edu (A.M. Abdulaziz).

https://doi.org/10.1016/j.ejpe.2019.08.005
1110-0621/

Thus, calculations of petrophysical uncertainty are identified as a chief analysis towards the development of accurate reservoir models [19]. The uncertainty analysis using probability density functions and Monte Carlo simulations could be essential in well test analysis. The pressure and rate of measurement reported the main errors that lead to major uncertainty in well test analysis [20] and the important input data for well test analysis can be constrained within an approximate uncertainty range. For example permeability-thickness product (kh) is usually known within 15%, the permeability (k) within 20%, the wellbore storage constant (C) within 20%, the skin factor (S) within ±0.3, and distances within 25% [20].

Discovered in 1973 with 43 billion barrel of proven reserve, West Al Qurna is one of the important Iraqi Oil Fields that produces from three oil-bearing zones within the Cretaceous succession; Saadi, Mishrif, and Yamama formations [21]. Virtually, this oil field produces only from the Mishrif pay zones with a daily production of approximately 450,000 barrel [22]. The petrophysics of Mishrif formation have been described using log and core data to identify criteria of the barriers within Cretaceous Mishrif formation of West Al Qurna Oil Field [23–26]. Based on well log interpretation in West Al Qurna Oil Field, Mishrif formation is characterized into flow units identified within three subunits; MA (3 flow units), MB1 and MB2 (10 flow units) [27]. Seismic data with well logs in south Iraq Oil Fields (West Al Qurna, Majnon, Nahr Umr, Zubair, and Rumaila) are integrated to build one dimensional petro-mod model for hydrocarbon characterization and modeling of the Early Cretaceous and Late Jurassic source rocks in the Basra Oil Fields [28].

Since the early stages of petroleum industry, several advances including analytical solution, pressure derivative, and deconvolution have been developed to improve well test analysis and interpretation [29–33]. Recent deconvolution methods [34–38] are investigated using field case studies and the results recognized the importance of deconvolution as an important tool for analysis and interpretation [39]. The best practice in well test, using ten years-long of worldwide research and experience, highlighted the need of gaining skills and clarifying the ambiguity in some well test concepts to get better results and develop easy well test procedures [40]. Well test analysis has five main sources of uncertain parameters with several degrees of importance and resolvability, including pressure data, flow rate, ambiguous response due to insufficient duration, parameter estimation, and uncertain reservoir properties [41]. The effect of errors in flow rate data on well test interpretation is evaluated using simultaneous analysis and the results showed a great reduction in the degrees of interpretation freedom, disappearance of wellbore storage effect, and complete vanishing of interlayer flow [42–44]. In addition, the error bounds in well test analysis for the most common parameters involve permeability (K) and skin factor (S) [5]. In the present study, detailed investigations to the uncertainty in petrophysical parameters of the pay zones in West Al Qurna Oil Field is introduced to evaluate the influence of such parameters on well test interpretation.

2. Methods

To evaluate the effect of uncertainty in petrophysics on well test analysis, three wells (WQ-403, WQ-418, and WQ-423) with complete log and well test data from the West Al-Qurna Field are analyzed. To be consistent with other digital data, the analog logs in wells WQ-403 and WQ-418 are scanned and subsequently digitized, edited, and reviewed. In few cases, the data is filtered to get rid of false digitization errors. All log data analysis and calculations are completed using the relations presented in Table 1-upper.

Table 1
The list of equations for petrophysical calculation and PVT correlations used in the analysis.

Petrophysical parameter	Equations	Reference
Volume of clay	$V_{sh}=\frac{0.5\times I_{GR}}{1.5-I_{GR}}$	Stieber, 1970 [45]
Porosity	$??=??_{D1}+\frac{\Phi N1-\Phi D1}{1-\frac{\Phi N1-\Phi N2}{\Phi D1-\Phi D2}}$	Bertozzi et al., 1981[46]; Dewan, 1986 [47]
Water saturation	$\frac{1}{\sqrt{Rt}}=\left[\sqrt{\frac{\Phi eff^{m}}{a\ Rw}}+\frac{Vcl^{\left(1-\frac{vcl}{2}\right)}}{\sqrt{Rcl}}\right].Sw^{n/2}$	Poete, 2012 [8]; Schlumberger, 2013 [48]
Irreducible water	ϕ^{Q}x Irreducible water(Swir) = Constant	Buckles, 1965 [49]
Residual oil saturation	$Sor=Ko=\frac{162.2\ Qo\ Bo\ \mu o}{m\ h}$	Brandes and Farley, 1993 [50]

PVT Correlations for PTA

Inputs	Type of correlation used	Output
	Oil (correlations, Inputs & outputs)	
GOR (Scf/bbl)	Standing	P_b & R_s
GOR(Scf/bbl)=510, API=24.7 & $??_g$=0.7	Standing	B_o
API=24.7,Temp=154 F°	Vasques & Beggs	μ_o
R_s & B_o	Vasques & Beggs	C_o
Water (correlations, inputs & outputs)		
Salinity=170kppm	Spivey	B_w
Salinity=170kppm	Dodson & Standing	C_w
Salinity=170kppm	Katz	R_{sw}
Salinity=170kppm	Van-wingen & Frick	μ_w

After estimation of (Φ_{avg}, Sw_{avg}, Vsh_{avg}, N/G) for all pay zones, the distribution of the possible errors associated with the interpretation parameters are calculated. Using error distributions, Monte Carlo simulation randomizes these parameters and execute multiple simulations through the analysis shown in Fig. 1. Subsequently, the results of each simulation are gathered to be displayed in a distribution. For each parameter in a particular simulation, the shift in this parameter is calculated using a random number generated based on the CPU clock time [48]. Once a shift is randomly determined, several characteristics are determined such as shift type, shift distribution, and shift value (high and low). Sensitivity analysis evaluates the relative importance for each input parameter on the overall results error. Graphically, the Tornado plot displays individual relative importance for each input parameter in the error analysis. To calculate an error for a parameter in Monte Carlo analysis, two runs are executed; one with the parameter set to its low value and the other for its high value (with ±x value-standard deviation, typically 2 in Gaussian distributions) while all other parameters are kept with the default values [48]. The same input parameters utilized in Monte Carlo simulation analysis are handled in sensitivity analysis and the output can be displayed either graphically or in tables. All petrophysical analysis and calculations are completed using Interactive Petrophysics –IP V4.2 software [48,51].

Data analysis of a well test typically involves data processing, flow regime identification, reservoir / wellbore model specification, and post model analysis. In data processing, Saphir NL [52] is used for pressure transient analysis with quality control and quality assurance. Since PVT data is not available for the three wells in the West Al-Qurna Oil Field, a PVT model is generated with the available data from MDT using empirical correlations shown in Table 1-lower. Flow regime is identified using the extracted Δp and deconvolution [53]. To identify the suitable analytical model for a well test analysis, wellbore, well, reservoir, and boundary models are respectively assigned as constant, vertical limited entry, homogenous, and infinite. The post modeling output usually encompasses an estimate of important parameters including; initial pressure, various types of permeability, radius of investigation,

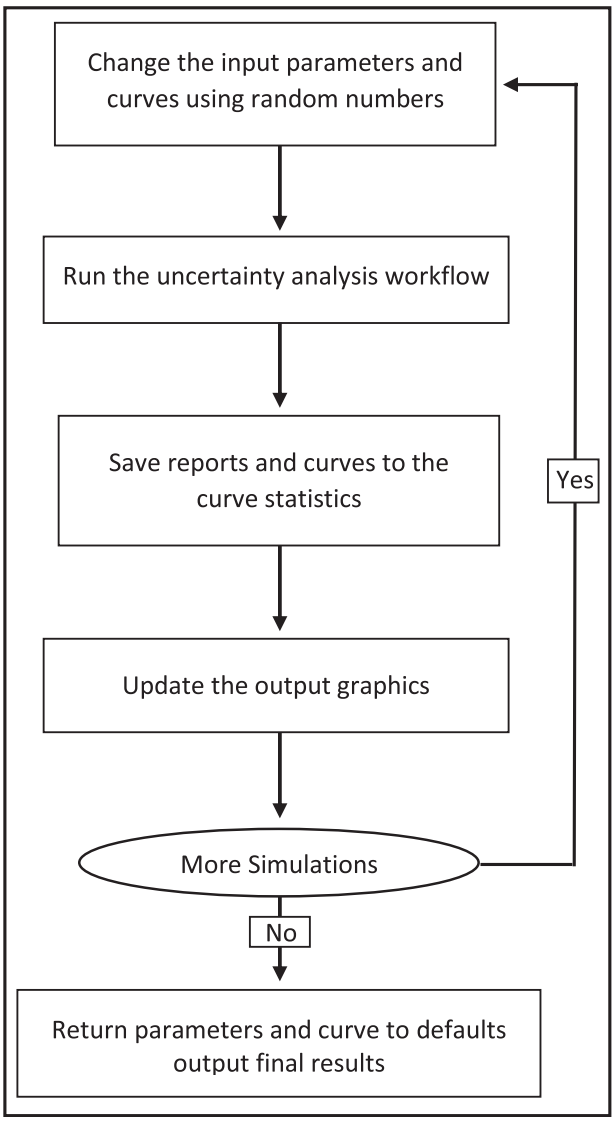

Fig. 1. The workflow applied in uncertainty analysis of petrophysical results.

and skin factor. Table 2 shows the mathematical relations of the analytical model applied in well test calculations. All well test analysis and interpretation are accomplished using Kappa-Workstation (V5.12 – 2016) [52].

Uncertainty of MDT data and sensitivity analysis is addressed and relationships are determined using similar approaches shown in Fig. 1. Bo and μo (derived from empirical correlation due to the lack of PVT data) are involved in the present uncertainty analysis as the only MDT downhole measurements. In addition, uncertainty in Net pay, φ, and Sw are considered in the present analysis for being influential in permeability, skin factor and radius of investigation calculations. To set up the simulation algorithm for uncertainty calculations, the distribution of each input parameter should be accurately identified. In the present study, the individual input parameters distribution is identified based on the histograms developed by petrophysics uncertainty and analogous applications. Generally, in the present analysis normal distribution is used for φ, Sw and μo while triangle distribution is used for net pay and box distribution is used for Bo. All uncertainty and sensitivity analysis are completed using VOSE 2016 of EXCEL plugin (Model risk VOSE, 2016) [55]. This plugin is developed for applications in business analysis and their internal codes were adjusted to fit a prediction model in petroleum industry. The developed codes are shown in Appendix A.

3. Results and Discussion

Several calculations have been made on well log records in West Al Qurna Field to reveal porosity, volume of clay, water saturation, and net/gross ratio. The petrophysical investigation of the studied wells (WQ-423, WQ-403 and WQ-418) penetrating Saadi and Mishrif formations involves petrophysical characterizations, uncertainty analysis, and sensitivity analysis.

3.1. Petrophysics of Mishrif and Saadi formations

The present analysis identified four main pay zones in Saadi and Mishrif formations based on representative cutoffs ($\phi = 0.15$, Sw = 0.40, and Vsh = 0.40). The Saadi pay zone represents the first pay zone and the other three pay zones (from top to bottom MA, MB1, and MB2) fall in Mishrif formation. All these pay zones are represented in well WQ-418 but only three zones are reported in wells WQ-403 and WQ-423. Saadi pay zone has not been seen in well WQ-403 while MB1 zone is not reported in well WQ-423. The Saadi pay zone thickness varies between 21.3 and 22.4 m, while MA pay zone falls between 24.8 and 27.6 m. MB2 showed a comparable thickness to the sedimentary units seen in MA with a thickness ranging between 25.3 and 26.3 m. The MB1 pay zone showed a relatively thin that typically reports less than 10 m thick. Fig. 2 shows an example for petrophysical interpretation on a Triple Combo display for well WQ-418 that presents a suit of input log data set and the interpreted reservoir characteristics. Using the available records of photoelectric effect and sonic logs, a reliable lithological identification, using the carbonate model, is developed for both Mishrif and Saadi formations. The Saadi formation is separated from Mishrif by a massive shaly limestone unit that usually has a shale content greater than 20%. Results showed that both Saadi and Mishrif formations are clean calcareous formations (shale content less than 4%) with limestone content greater that 70% and dolomite content between 10 and 20%. For each pay zone or reservoir interval in all wells, the Monte Carlo Simulation analysis provides a set of outputs including tabulated values, histograms, and cross plot for each property involved in reservoir characterization. The tabulated values involve the probability 10, 50, and 90% (output percentiles). A summary of important

Table 2
Equations of the analytical model applied in pressure transient analysis.

Equation #	Parameters	Equations	Reference
1	K_o (mD)	$Ko = \frac{162.2\ Qo\ Bo\ \mu o}{m\ h}$	[29]
2	K_w (mD)	$Kw = \frac{162.2\ Qw\ Bw\ \mu w}{m\ h}$	[29]
3	K_{abs} (mD)	$K_{abs} = \frac{Ko}{Kro}$ or $K_{abs} = \frac{Kw}{Krw}$	[29]
4	R_{inv} (m)	$(Rinv) = 0.029\ \sqrt{\frac{k\Delta t}{\phi \mu ct}}$	[54]
5	Skin Factor	$S = 0.5\ \left[\frac{Pi - P1hr}{m} - \ln\frac{k}{\phi\ \mu\ ct\ rw^2} - 0.80907\right]$	[54]

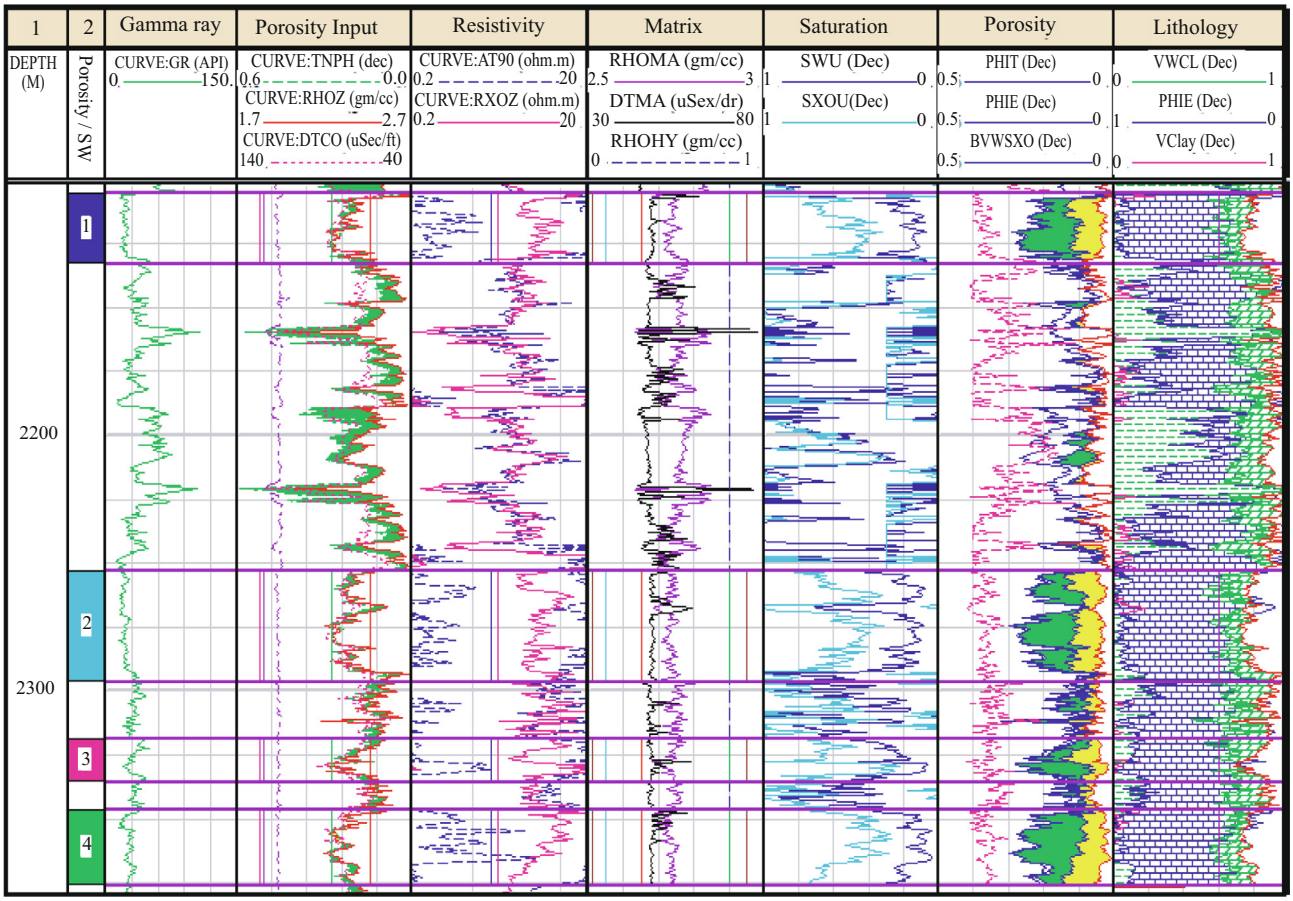

Fig. 2. An example to the petrophysical interpretation for well WQ-418.

Table 3
The output percentiles (P10, P50, and P90) of uncertainty analysis for the petrophysical results.

Well	Zone	Depth (m)	Prob. (%)	Pay Thick (m)	Net/Gross	??$_{Avg}$	S_w	V_{Clay}	
		From	To						
423	Saadi	2103.8	2133.1	10	15.2	0.52	0.205	0.182	0.1
				50	21.2	0.72	0.219	0.142	0.07
				90	25.8	0.88	0.236	0.093	0.027
	MA	2256.13	2292.6	10	4.0	0.11	0.211	0.141	0.12
				50	26.2	0.72	0.226	0.112	0.07
				90	33.2	0.91	0.248	0.080	0.001
	MB2	2347.1	2376.4	10	13.3	0.44	0.221	0.102	0.147
				50	23.3	0.78	0.237	0.075	0.106
				90	27.8	0.93	0.258	0.048	0.045
403	MA	2256.6	2289.7	10	17.5	0.53	0.216	0.278	0.051
				50	26.4	0.80	0.229	0.236	0.022
				90	30.9	0.94	0.244	0.195	0.001
	MB1	2322.9	2334.7	10	6.4	0.54	0.208	0.25	0.034
				50	7.6	0.64	0.222	0.212	0.023
				90	8.8	0.74	0.235	0.178	0.012
	MB2	2349.1	2376.2	10	17.5	0.64	0.233	0.197	0.041
				50	22.9	0.85	0.244	0.159	0.029
				90	26.0	0.96	0.26	0.119	0.012
418	Saadi	2105.1	2132.6	10	15.1	0.55	0.22	0.169	0.065
				50	22.3	0.81	0.231	0.143	0.031
				90	23.8	0.86	0.247	0.113	0.001
	MA	2252.3	2286.12	10	9.8	0.29	0.213	0.175	0.065
				50	24.8	0.73	0.229	0.146	0.027
				90	29.6	0.88	0.249	0.107	0.001
	MB1	2322.6	2336.0	10	4.3	0.32	0.21	0.165	0.069
				50	9.5	0.71	0.224	0.133	0.048
				90	10.6	0.79	0.253	0.081	0.007
	MB2	2347.11	2376.37	10	14.8	0.51	0.221	0.143	0.054
				50	26.2	0.90	0.233	0.116	0.033
				90	27.9	0.95	0.253	0.08	0.009

petrophysical parameters in these results is presented in Tables 3. Results of uncertainty analysis (P10, P50, and P90) in all wells showed virtually consistent values in most petrophysical parameters of reservoir results, but such consistency is dramatically changed in pay results. Among different reservoir parameters, Φ_{AVG} and Vclay showed relatively consistent values calculated under different probabilities, reflecting the nature of steady and stable environment of deposition (Table 3). However, a major discrepancy and variations is obvious in pay thickness and N/G calculations under different probabilities. Nearly all zones in pay results showed a considerably varying results under different probabilities, but such variations are minimized in MB1 zone, particularly those defined in well WQ-403 (Table 3). Generally, all studied wells are characterized by consistent facies, and this is confirmed by good consistent mean values of net pay zones in both uncertainty analysis and log interpretation (e.g. 22.3 m for uncertainty and 22.4 for log interpretation of Saadi formation in well WQ-418, Table 3). Among the items entailing a significant uncertainty is the N/G that exhibited an obvious instable calculation in the net pay results MA zone in wells WQ-423 and WQ-403. For examples, in the MA zone of well WQ-423, the N/G calculations varied between 0.10 (at P10) and 0.91 (at P90) whereas in zone MA of well WQ-403, the N/G calculated values varied between 0.53 (at P10) and 0.93 (at P90) (Table 3).

Porosity calculations under uncertainty in the West Al Qurna Oil Field provides slightly higher estimates in the average porosity compared to the corresponding average calculated by the conventional log analysis. These differences in the mean porosity value typically fall within 1% in Saadi pay zone, but report approximately 3% in the pay zones of the Mishrif formation. Such results are consistent with the Vclay calculations in both Saadi and Mishrif formations. The uncertainty analysis of all pay zone results at 10, 50, and 90 percentiles (Table 3) provides a relatively consistent average porosity values that typically fall between 20 and 26%. Compared to the conventional log analysis, Sw calculations under uncertainty showed different trends in the calculated average water saturation. The variations in average value between uncertainty analysis and log analysis do not exceed 2.6% as reported in MA zone, but the

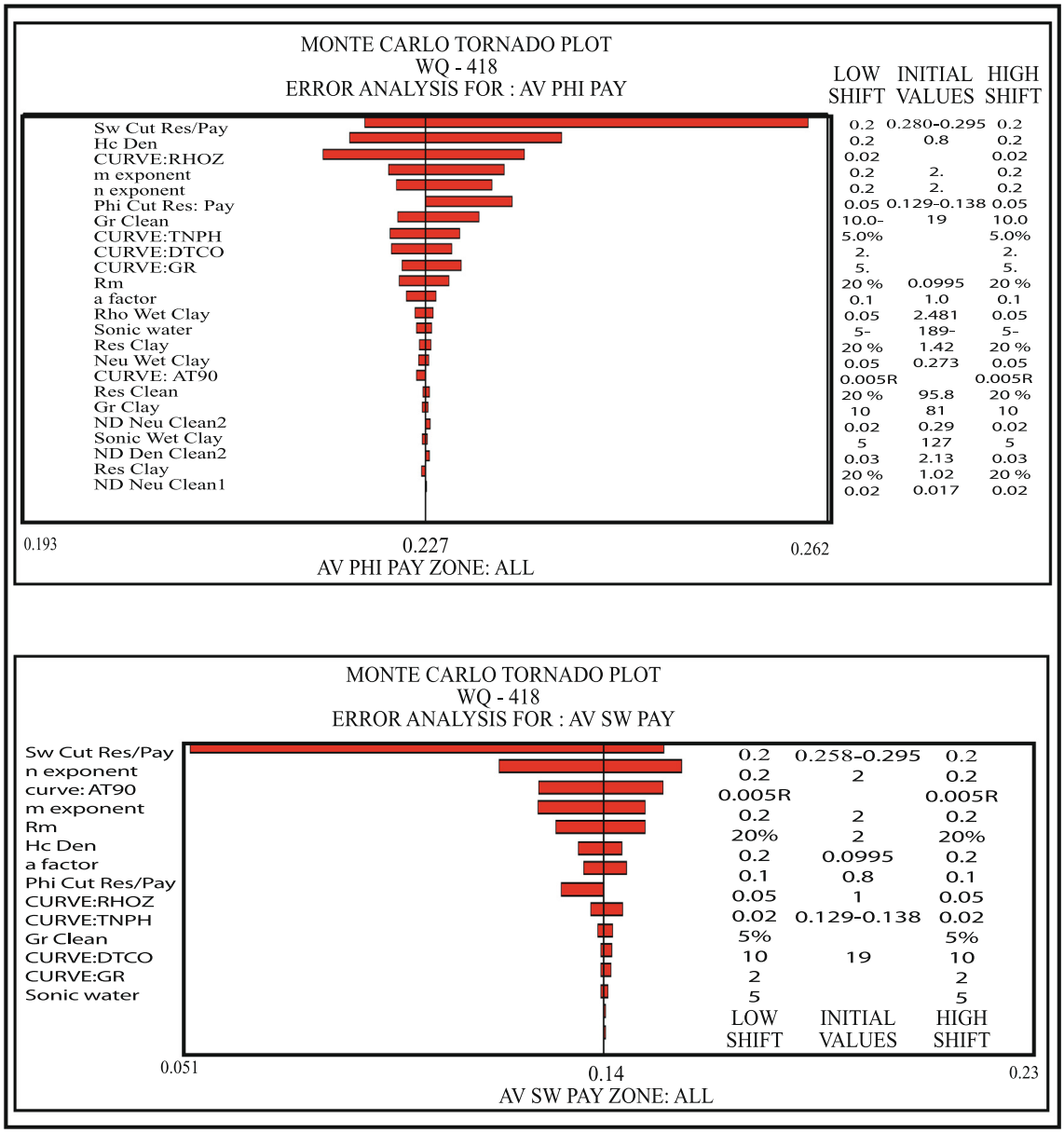

Fig. 3. The Tornado plot for average porosity (upper) and average Sw (lower) calculations in well QW-418.

common change typically falls below 0.8% as seen in both Saadi and MB1(Table 3). In general, the discrepancies in the average Sw value between log analysis and uncertainty analysis increases when the change in various probabilities (P10, P50, and P90) fall between 3 and 4%, as calculated in wells WQ-423 and WQ-403 (Table 3). In all cases, the calculated Sw in all pay zones significantly fall below 30% and the majority fall close to 18% in the delineated pay zones of all wells under different probabilities. This indicates a relatively consistent Sw through the pay zones, but this does not hinder its effect on sensitivity analysis as well. The uncertainty in shale content represents a proficient benchmark to indicate the stability of depositional environment of a specific formation. Generally, the volume of clay rarely exceeds 10% in most pay zones of the studied wells with MB1 and MB2 pay zones showing relatively higher shale content compared to other zones in well WQ-418. The maximum Vclay is calculated in MB2 pay zone of well WQ-418 and reporting 13% that still keeps the lithology as clean formation (Fig. 2).

Model uncertainty is typically dependent to the selection of appropriate interpretation model that best describes the system. In the present study, cutoffs delineating the pay zones could be an important factor that control N/G accuracy based on input log measurements. Tornado plot is dominantly applied in uncertainty analysis to identify weights of the input parameters in calculation errors of output interpretation results. Fig. 3-upper presents the Tornado plot constructed for average porosity calculations of the pay zones in well WQ-418, and indicates that the calculations are significantly influenced by Sw cutoffs, but could be affected by hydrocarbon density, density log measurements, and some Archie parameters (m and n). Alternatively, Sw calculation is significantly affected by Sw cutoff and deep resistivity measurements, but Archie parameters and Rw may represent important influences (Fig. 3-lower). The volume of clay calculations seems strongly sensitive to the clean Gamma ray, Sw cutoff, and Gamma ray records, but secondary influences can be attributed to deep resistivity measurements and Archie parameters. In N/G calculations the Sw cutoffs showed the major influence on the calculated N/G values, but an intermediate influences are attributed to Archie parameters (a, m, and n) and porosity logs (density and neutron). The secondary influences are reserved to Rw, deep resistivity, and sonic logs.

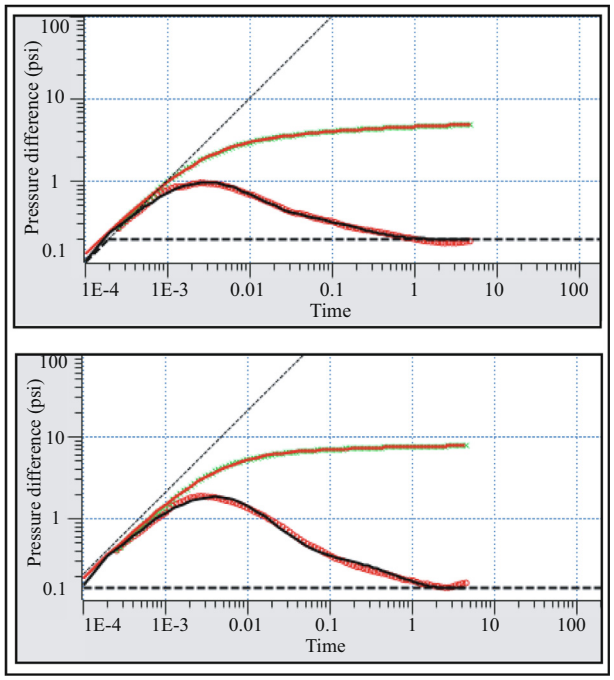

Fig. 4. Pressure derivative plot for MA (upper) and MB2 (lower) pay zones of Mishrif formation in well WQ-418.

3.2. Well test interpretation

Pressure analysis showed a perfect radial flow regime achieved in Saadi and MA zones (e.g. Fig. 4-upper) but the achieved radial flow in MB2 zone has associated decreased time near the end of record (Fig. 4-lower). Compared to the measured pressure, interpreted pressure data in all wells are relatively match-able, particularly in Saadi and MA zones, but MB2 zone showed a slight misfit (-6 psi) that could be induced by data analysis. Permeability estimates including Ko, Kw, Kro, Krw, and Kabs are calculated using equations 1, 2 and 3 (Table 2) and the results for all studied wells are shown in Table 4. The Kro and Krw of Saadi, MA, and MB2 zones in all wells can be determined using Stone II method with the aid of the Kro/Krw versus Sw plot. Generally, Saadi zone reported very low permeability values (Kabs ~1 mD) that confirms the long-time of oil withdrawal and shale lamination recognized in well log analysis. However, both MA and MB2 zones showed moderate estimates of permeability; Kabs is approximately 36 mD in MA and 56 mD in MB2 zones (Table 4). The high permeability observed in MB2 could be related to well-developed secondary porosity as shown in porosity measurements of well log analysis and the dual porosity pattern identified Fig. 4-lower. Equation 4 calculates the radius of investigation (Rinv). Table 4 shows limited radius in Saadi (3 m) compared to the calculated radius in MA (11 to 20 m) and MB2 (15 to 22 m). This observation confirms the calculated permeability and porosity in all zones. The calculated skin factor (Table 4) reported a relatively moderate positive skin at Saadi and MB2 zones (+1) that confirms the LFA results, but MA zone showed value fall below the +1.

The results of well test uncertainty analysis (mean value and output percentiles: 10, 50, and 90%) to all pay zones in the studied wells are presented in Table 5. In a general sense, the P50 results in all calculated parameters (K, Rinv, and skin factor) are highly correlated with the conventional calculations in well test that usually

Table 4
The results of pressure test analysis for all wells.

Well	Formation	Conventional well test results					Additional results				
		Ko (mD)	Kw (mD)	Kabs (mD)	Rinv (m)	Skin	Ko/Kw	Kro	Krw	Sw log	Sw (St)
WQ-418	Saadi	0.67	0.018	0.9	3.01	1.01	37.2	0.7381	0.0198	0.148	0.149
	Ma	30.91	0.891	36.6	19.77	0.25	34.69	0.8443	0.0243	0.148	0.148
	MB2	45.01	1.18	52.63	22.29	1.03	38.14	0.8551	0.0224	0.124	0.124
WQ-403	Ma	34.45	0.9111	40.33	12.07	0.85	38.81	0.8542	0.0225	0.241	0.244
	MB2	46.8	1.369	55.53	15.67	0.79	34.18	0.8426	0.0246	0.166	0.166
WQ-423	Saadi	0.425	0.0121	0.584	2.49	3.62	33.73	0.7278	0.0215	0.148	0.149
	Ma	27.92	0.727	32.62	11.54	0.62	38.4	0.8558	0.0222	0.117	0.117
	MB2	48.66	1.237	56.68	15.22	0.25	39.33	0.8584	0.0218	0.085	0.858

Table 5
The results of well test uncertainty analysis (mean value and output percentiles: 10, 50, and 90%) to all pay zones of the studied wells.

Wells	Formations	P	Ko(mD)	Kw(mD)	Kabs(mD)	Rinv(m)	Skin
WQ-418	Saadi	Base Case	0.67	0.018	0.9	3.01	1.01
		Mean	0.7	0.0188	0.94	3.02	1.05
		P10	0.62	0.0167	0.84	2.91	1.01
		P50	0.68	0.0183	0.92	3.02	1.05
		P90	0.8	0.0216	1.08	3.14	1.1
	Ma	Base Case	30.91	0.891	36.6	19.77	0.25
		Mean	31.82	0.9233	37.74	19.16	0.22
		P10	26.9	0.79	31.98	18.18	−0.19
		P50	31.21	0.9	36.96	19.15	0.2
		P90	37.36	1.08	44.26	20.15	0.65
	MB2	Base Case	45.01	1.18	52.63	22.29	1.03
		Mean	46.36	1.2267	54.28	22.13	1.01
		P10	39.19	1.04	45.9	21.03	0.87
		P50	44.59	1.17	52.15	22.06	1.02
		P90	55.3	1.47	64.78	23.32	1.16
WQ-403	Ma	Base Case	34.45	0.9111	40.33	12.07	0.85
		Mean	36.81	0.9733	43.09	12.47	0.79
		P10	30.77	0.82	36.06	11.8	0.42
		P50	35.91	0.95	42.04	12.42	0.78
		P90	43.76	1.15	51.19	13.2	1.18
	MB2	Base Case	46.8	1.369	55.53	15.67	0.79
		Mean	49.31	1.4433	58.52	15.5	0.78
		P10	40.82	1.2	48.47	14.57	0.7
		P50	47.18	1.38	55.99	15.49	0.78
		P90	59.94	1.75	71.11	16.45	0.86
WQ-423	Saadi	Base Case	0.425	0.0121	0.584	2.49	3.62
		Mean	0.44	0.013	0.672	2.68	2.81
		P10	0.38	0.0113	0.452	2.5	2.75
		P50	0.43	0.0127	0.511	2.66	2.81
		P90	0.51	0.015	0.902	2.88	2.89
	Ma	Base Case	27.92	0.727	32.62	11.54	0.62
		Mean	32.86	0.8666	38.45	10.8	0.61
		P10	21.17	0.5512	24.72	9.42	0.43
		P50	27.65	0.721	32.3	10.75	0.63
		P90	49.76	1.3372	58.33	12.25	0.78
	MB2	Base Case	48.66	1.237	56.68	15.22	0.25
		Mean	49.76	1.2767	58.03	15.42	0.153
		P10	41.4	1.0514	48.2	14.48	0.07
		P50	48.01	1.2285	55.91	15.35	0.15
		P90	59.9	1.5672	69.98	16.44	0.24

adopt average value rather than using probability analysis. However, the other probabilities (P10 and P90) show significant changes in all calculated parameters justifying the importance of uncertainty analysis. Among the various parameters presented in Table 5, the effective permeability, radius of investigation, and skin factor represent the most influential well test results. In Saadi zones, all calculated parameters under uncertainty did not show marked changes as compared to conventional results. This typically stands true for all tight oil reservoirs where the changes in estimated parameters under uncertainty hardly exceeds 10% in most parameters, typically less than 1 mD in Kabs for example. The Kabs of Saadi zone typically reports a range of calculated values between 0.45 and 1.08 mD in all wells, while the Rinv remains within a range of 2.5 – 3.14 m (Table 5). The calculated skin factor in Saadi zones showed similar behavior in individual wells but the calculated skin in well WQ-423 is almost 2.7 times the calculated skin in well WQ-418 indicating considerable damage in well WQ-423.

In MA zone, the calculated P90 of Kabs showed significant changes compared to the conventional calculations. For example, the conventional calculations in well WQ-423 yields Kabs 32.3 mD while the P90 Kabs provides 58.3 mD indicating 44% increase. This effect is decreased to approximately 17% difference between the P50 and P90 in other wells, P50 = 42 mD, P90 = 51 mD for well WQ-403, and P50 = 36.9 mD, P90 = 44.3 mD for well WQ-418. These marked changes in Kabs from well WQ-423 to the other wells can be attributed to the high uncertainty in pay thickness calculations of well WQ-423 where the P50 of the pay thickness reported 26 m while the P90 was 33 m. In contrast, the Rinv in MA zones showed moderate changes (~1.0 m representing 10% change) between the conventional Rinv calculations and the P90 values of uncertainty analysis. Generally, the highest estimated Rinv is reported in well WQ-418 where the various probabilities fall between 19 and 20 m. The maximum change in Rinv of MA zone is recorded in well WQ-423 where the P50 and P90 estimates are 10.75 m and 12.25 m respectively. The other wells showed approximately similar changes, (P50 = 12.4, P90 = 13.2 for well WQ-403 and P50 = 19.1, P90 = 20.15 for well WQ-418) (Table 5). The uncertainty analysis in MA zone generally showed acceptable skin effect in all wells that typically ranges between −0.78 in well WQ-418 to 1.18 in well WQ-403. The minimal differences in calculated probabilities of skin effect in MA zone is encountered in well WQ-423 (P50 = 0.63 and P90 = 0.78) while the significant variation is seen in well WQ-418 (P50 = 0.2 and P90 = 0.65) (Table 5).

MB2 zones showed the highest Kabs among the developed zones in all wells with calculated values range between 45.9 mD (P10 in well WQ-418) and 71 mD (P90 in well WQ-403) (Table 5). The calculated probabilities (P10, P50, and P90) in each well showed relatively similar differences (20% difference between conventional Kabs calculations and P90 values). However, the corresponding values could moderately vary to report from as low as 12.6 mD in well WQ-418 to 15.1 mD in well WQ-403. The radius of investigation calculated in MB2 zone showed the greatest values among the studied zones and varies between 14.5 m (P10 in well

WQ-423) and 23.3 m (P90 in well WQ-418) (Table 5). However, the calculated Rinv using conventional methods (P50) typically varies from P90 in MB2 zone of all wells to approach 1.25 m. This could be due to the accurately defined pay thickness, and therefore the calculated uncertainty was minimal. Generally, the skin factor calculated in MB2 zone fall below 1 with the minimal skin (P50 = 0.15 and P90 = 0.24) in well WQ-423, while the higher skin is encountered in well WQ-418 with P50 = 1.0 and P90 = 1.16.

3.3. Sensitivity analysis to well test calculations

A Tornado plot is designated to estimate the impact of each input parameter on the output result in a specific property calculation. Considering full probability region (P0 to P100), the sensitivity analysis for Ko, Kw, Radius of investigation and skin factor in all studied wells are presented in Table 5 and Tornado plots of well WQ-418, as a sample, are presented in Fig. 5. Generally, Ko and Kw calculations are strongly affected by uncertainty in pay thickness with minimal effect reported in Saadi zone of well WQ-418 and maximum effect in MA zone of well WQ-423 (Table 6 and Fig. 5). A medium effect to Ko and Kw calculations are typically

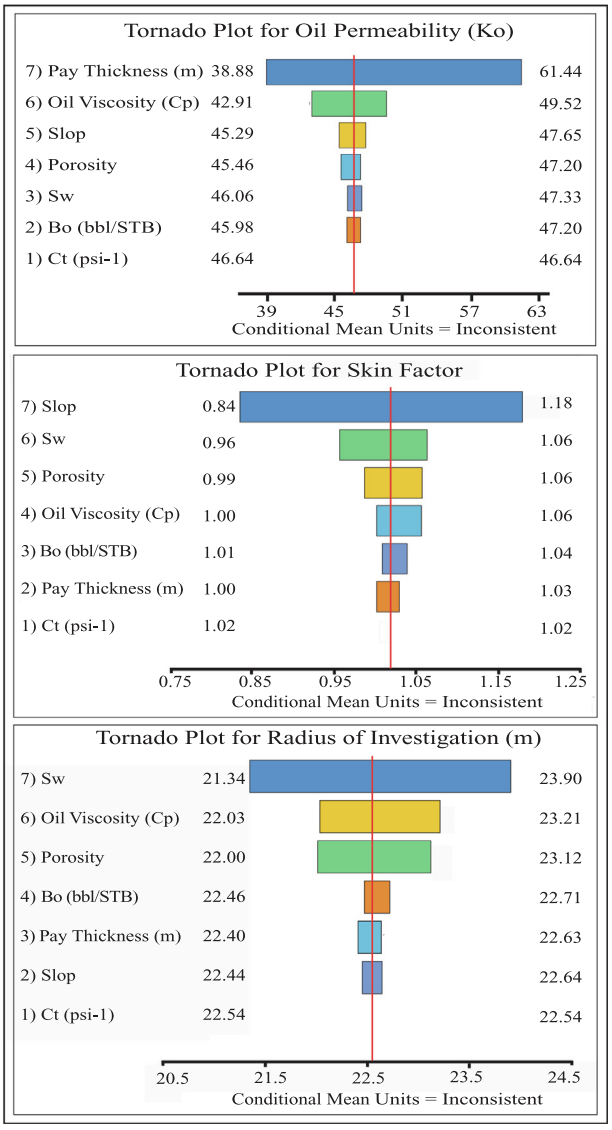

Fig. 5. The Tornado plot for oil permeability (upper), skin factor (middle), and the radius of investigation (lower).

Table 6
Error analysis results for all wells under full probability region (P0 to P100).

Wells	Formation	Parameters	Pay thick.	ϕ	Sw	μo	Bo	Pressure
			(%)					
WQ-418	Saadi	Ko	19	3	5.4	5	4	6
		Kw	14.5	3.6	5.6	4.6	4.1	5.5
		Rinv	0.3	2	4.4	0.4	0.4	0.6
		Skin	1	2.5	5.3	1	0.7	4
	MA	Ko	22	3	4.2	9	5	10
		Kw	21	3	2.8	2.6	4.5	13.3
		Rinv	1	2.5	5.5	2.3	0.8	1
		Skin	15	16	20	15	20	40
	MB2	Ko	26	5.7	2.7	9	2	7.5
		Kw	21	2.3	1.9	7	2.4	6
		Rinv	2.5	3.5	8	5	2.8	2
		Skin	1	3	4	2	1	13.5
WQ-403	MA	Ko	24	2.7	2	6	2.7	15
		Kw	20	4	3	1.5	4	11
		Rinv	0.6	2	8	3.6	0.4	0.5
		Skin	4	5	8	5	6	36
	MB2	Ko	29	5	8	9	8.7	7.7
		Kw	30	4	9	7	10	9
		Rinv	1	3.5	7	2.5	1	1.5
		Skin	3	6	9.5	5	2.5	10
WQ-423	Saadi	Ko	18	3	1	5	2	1
		Kw	21	7.5	3	9	6	3
		Rinv	6	8.5	17	6	5	7.5
		Skin	0.9	2	4.4	1	0.6	1.8
	MA	Ko	47	3	2	1.2	2	1
		Kw	26	6	5	2	4	3
		Rinv	2	4	16	5	1	2
		Skin	2	8	11	5	2	17
	MB2	Ko	30	5	3.5	9	6	5
		Kw	28	5.6	4.9	6	7.5	6
		Rinv	3	5	9	4	3	3
		Skin	7	18	3.2	10	8	30

attributed to μo, Φ, and pressure measurements (Table 6). Despite the remarkable uncertainty in the petrophysical parameters calculated in Saadi pay zones, it induces insignificant changes in the calculated values of the well test results. This is probably due to the tight conditions prevailing Saadi formation (Table 6). Alternatively, the radius of investigation calculations are affected mainly by Sw that typically changes the Rinv to 1.5 m in MB2 zone of well WQ-418 (Fig. 5), with major influences depicted in MA zone (Rinv = 2.0 m) of well WQ-423 (Table 6). A secondary effect on Rinv calculations (~0.70 m) is attributed to the uncertainty in porosity and μo. Skin factor calculations showed a great sensitivity to the pressure measurements that typically falls between 0.06 and 0.5. Secondary effects in skin factor calculations (0.1) are attributed to Sw and porosity uncertainty. Other parameters including oil formation volume factor and total compressibility showed insignificant effects on well test calculations (Fig. 5).

4. Conclusion

The present study evaluated the effect of uncertainty in petrophysics and fluid properties on well test results. The N/G uncertainty analysis in the studied wells showed relatively similar effects at various probabilities in the Saadi pay zones, but reported large differences in most pay zones of Mishrif formation. Uncertainty of porosity calculations in West Al Qurna Oil Field tends to provide a slightly higher estimate in the average porosity value compared to the corresponding average values derived by conventional log analysis. The Sw values change moderately in various probabilities (P10, P50, and P90) and typically fall between 3 and 4%. In well test analysis, the effective permeability calculations (14.5% and 47%), are strongly affected by the pay thickness uncertainty in Mishrif formation, with medium influences induced by

pressure (∼10%), μo & Bo (∼9%), Φ(∼6%), and Sw (∼5%). Radius of investigation calculations are affected mainly by Sw (∼9%) and porosity (5%) uncertainties, with minimal influence by Bo, μo, and pressure. The skin factor calculations showed a great sensitivity towards the pressure measurements with changes in results falling close to 35%. Results indicated that Saadi zone is extremely tight and do not show significant responses to uncertainty effect to both lithological and fluid properties. Alternatively, marked differences in outputs of conventional and uncertainty analysis well test are reported in Mishrif formation (MA and MB2 pay zones) indicating the importance of incorporating petrophysics uncertainty in well test analysis of permeable formations.

Appendix A

Random number generation in ModelRisk

Model Risk uses the Mersenne Twister to generate random numbers for its simulation functions. Mersenne Twister is a pseudo-random number generating algorithm developed by Makoto Matsumoto and Takuji Nishimura in 1997 and refined in 2002. It has passed all of the most rigorous random number tests and registered a very significant improvement over all previous generators.

The Mersenne Twister has the following merits:

- It is designed with consideration on the flaws of various existing generators;
- It offers a far longer period and far higher order of equidistribution1 than any other implemented generators. (It has been proven that the period is (2^19937)-1, and 623-dimensional equidistribution property is assured);
- Fast generation. It is as fast as the standard ANSI-C library in a system with pipeline and cache memory;
- Efficient use of the memory. (The code implemented in C++ consumes only 624 words of working area.):

$$\lim_{x\to\infty}\frac{|\{s_1,\ldots,s_n\}\cap[c,d]|}{n}=\frac{d-c}{b-a}$$

Distributions
Sub Test ()
Dim Result **As Variant**, Min **As Variant**, Mode **As Variant**, Max **As Variant**
Min = 1
Mode = 3
Max = 5
Result = ModelRisk.VoseTriangle(min, mode, max)
Debug.Print result
End Sub
Sub Test ()
Dim Result **As Variant**, Mu **As Variant**, Sigma **As Variant**
Mu = 0
Sigma = 1
Result = ModelRisk.VoseNormal(mu, sigma)
Debug.Print result
End Sub 2
Probability
Sub Test()
Dim result **As Variant**, X **As Variant**, Min **As Variant**, Mode **As Variant**, Max **As Variant**, Cumulative **As Variant**

Random number generation in ModelRisk (*continued*)

Distributions
X = Array(3.027,2.532,3.975,2.551,3.732)
Min = 1
Mode = 3
Max = 5
Cumulative = **False**
Result = ModelRisk.VoseTriangleProb(x, min, mode, max, cumulative)
Debug.Print result
End Sub
Sub Test()
Dim Result **As Variant**, X **As Variant**, Mu **As Variant**, Sigma **As Variant**, Cumulative **As Variant**
X = Array(−0.228, −1.393, −0.595,0.856,0.35)
Mu = 0
Sigma = 1
Cumulative = **False**
Result = ModelRisk.VoseNormalProb(x, mu, sigma, cumulative)
Debug.Print result
End Sub
Fitting method
Sub Test()
Dim Result **As Variant**, data **As Variant**, uncertainty **As Variant**, u **As Variant**
X = Array (−0.228, −1.393, −0.595, 0.856, 0.35)
Result = ModelRisk.VoseNormalFit(x)
End Sub
Visual Basic
Public Enum MR_ResultChartType
LIST_CHART = 1
HISTOGRAM_CHART = 2
CUMULA_CHART = 3
CUMULD_CHART = 4
BOXPLOT_CHART = 5
SCATTER_CHART = 6
SPIDER_CHART = 7
TORNADO_CHART = 8 3
SUMMARY_CHART = 9
STATISTICS_CHART = 10
PARETO_CHART = 11
End

Members	Description
LIST_CHART = 1	List of sampled values
HISTOGRAM_CHART = 2	Histogram chart
CUMULA_CHART = 3	Cumulative Ascending chart
CUMULD_CHART = 4	Cumulative Descending chart
BOXPLOT_CHART = 5	Box-plot chart
SCATTER_CHART = 6	Scatter chart
SPIDER_CHART = 7	Spider chart
TORNADO_CHART = 8	Tornado chart
SUMMARY_CHART = 9	Summary chart
STATISTICS_CHART = 10	Output statistics
PARETO_CHART = 11	Pareto chart

References

[1] J.O. Amaefule, D.G. Kersey, D.M. Marschall, J.D. Powell, L.E. Valencia, D.K. Keelan, SPE paper # 18167 presented in Annual Technical Conference and Exhibition, 2-5 October, Houston, Texas (1988), https://doi.org/10.2118/18167-MS

[2] D.G. Harris, C.H.J. Hewitt, Pet. Tech. (1977) 761–770, https://doi.org/10.2118/6109-PA.

[3] R.M. Sneider, H.R. King, H.E. Hawkes, T.B.J. Davis, Pet. Tech (1983) 1725–1734, https://doi.org/10.2118/10072-PA.

[4] M.M. Ibrahim, A.M. Abdulaziz, K.A. Fattah, Egypt J. Pet. 27 (4) (2018) 887–896, https://doi.org/10.1016/j.ejpe.2018.01.004.

[5] A.C. Gringarten, SPE Res. Eval. Eng. 11 (1) (2008) 41–62, http://dx.doi.org/10.2118/102079-PA.

[6] F.G. Paul, C. Luca, SPE-84387 paper presented in SPE Annual Technical Conference and Exhibition, 5-8 October, Denver, Colorado, (2003) 1-16. https://doi.org/10.2118/84387-MS

[7] E. Pasternak, Search and Discovery Article #120011, in: presented at AAPG Geoscience Technical Workshop on Reserves Determination (2009).

[8] N. Poete, SPWLA-Kuwait Chapter-2011-2-12, Session, Kuwait, May 15th, 2012. Online resource accessed on 10/12/2016, http://www.spwla-kuwait.com/pdf/tech-lib/May2012_1_Quantitative_Petrophysical_Uncertainty_public.pdf

[9] L. Mohamed, V. Christie, M.A. Demyanov, SPE Journal 15(1) (2010) 31– 38, SPE 119139, https://doi.org/10.2118/119139-PA.

[10] J.R. Hook, SPWLA-1983-Y, Society of Petrophysicists and Well-Log Analysts (SPWLA), 1983.

[11] D.B. Hertz, Harvard Business Rev. 42 (1) (1964) 95–106, https://hbr.org/1979/09/risk-analysis-in-capital-investment.

[12] J.E. Walstrom, T.D. Mueller, R.C. McFarlane, JPT (1967) 1595–1603, https://doi.org/10.2118/1928-PA.

[13] H.C. Chen, J.H. Fang, SPWLA-1986-vXXVIIn5a3, Society of Petrophysicists and Well-Log Analysts, 1986, pp. 39–44 (ISSN: 0024-581X).

[14] M.M. Ibrahim, A.M. Abdulaziz, K.A. Fattah, SPE paper # SPE-183565-MS presented in Abu Dhabi International Petroleum Exhibition and Conference, 7-10 November, Abu Dhabi, UAE (2016), https://doi.org/10.2118/183565-MS

[15] S.J. Adams, SPE-93125. SPE paper # 93125-MS presented in SPE Asia Pacific Oil and Gas Conference and Exhibition, 5-7 April, Jakarta, Indonesia (2005). https://doi.org/10.2118/93125-MS

[16] Z. Komlosi, J. Komlosi, SPE paper #121256 presented in EUROPEC/EAGE Conference and Exhibition, 8-11 June, Amsterdam, The Netherlands. (2009). https://doi.org/10.2118/121256-MS

[17] G. Samotorova, SPE paper # 171211-RU presented in SPE Russian Oil and Gas Exploration & Production Technical Conference and Exhibition, 14-16 October (2014) Moscow, Russia. https://doi.org/10.2118/171211-RU

[18] D. Viberti, F. Verga, M.T. Galli, P. Gossenberg, 2007-095 Offshore Mediterranean Conference.(OMC) Paper – Offshore Mediterranean Conference and Exhibition, 28-30 March, 2007, Ravenna, Italy. (ISBN: 9788894043624)

[19] S.O. Stalheim, Society of Petrophysicists and Well-Log Analysts. SPWLA 57th Annual Logging Symposium, 25-29 June (2016), Reykjavik, Iceland

[20] A.C. Azi, A. Gbo, T. Whittle, A.C. Gringarten, SPE-113888 presented at the Europe/EAGE Conference and Exhibition, 9-12 June (2008) Rome, Italy. https://doi.org/10.2118/113888-MS

[21] K.H. Alim, MSc thesis, Mid Sweden University, (2014) pp.79. An internet resource accessed on 12/2/2017: http://miun.diva-portal.org/smash/get/diva2:768346/FULLTEXT01.pdf

[22] G. Chon, The Wall Street Journal Retrieved (2009) 04–19.

[23] G.H. Sherwani, MSc thesis, Baghdad Univ., Iraq (in Arabic) (1983).

[24] A.A.M. Aqrawi, G.A. Thehni, G.H. Sherwani, B.M.A. Kareem, Iraq J. Petrol. Geol. 21 (1998) 57–82, https://doi.org/10.1111/j.1747-5457.1998.tb00646.x.

[25] S. Al-Jumaily, PhD thesis, Baghdad University, Iraq (2001) (in Arabic).

[26] A.J. Al-Khafaje, MSc thesis, Baghdad University, Iraq (2006) (in Arabic).

[27] H.A.F. Hassan, Master of Science Thesis in petroleum engineering, University of Baghdad, September, 2011.

[28] T.K. Al-Ameri, J. Pitman, M.E. Naser, J. Zumberge, H.A. Al-Haydari, Arabian J. Geosci., No.7-8 (2010) 1239–1259, https://doi.org/10.1007/s12517-010-0160-z.

[29] R.L. Perrine, New York, American Petroleum Institute (API) (1956) 482–550.

[30] H.J. Ramey, in: Proceedings of the 3rd Invitational Well-Testing Symposium, T. W. Doc, W.J. Schwarz, Eds., (1980) pp. 130–134, Berkeley, Calif, USA

[31] H.J. Ambastha, A.K. Ramey, Stanford U, SPE-24378-MS presented in SPE Rocky Mountain Regional Meeting, 18–21 May (1992). Casper, Wyoming. https://doi.org/10.2118/24378-MS.

[32] T. Ireland, J. Josef, An internet resource accessed on 20/1/2017, p. 58 (1992). https://www.slb.com/~/media/Files/resources/oilfield_review/ors92/0492/p46_57.pdf

[33] T. Ahmed, Gulf Professional Publishing, Elsevier, 30 Corporate Drive, Suit 400, Burlington, MA 01803, USA, (2006) p. 468. ISBN-13: 978-0750679725

[34] T. Von Schroeter, F. Hollaender, A.C. Gringarten, SPE-71574 presented at the SPE Annual Technical Conference and Exhibition, Sept 30 - Oct 3 (2001), New Orleans, USA. https://doi.org/10.2118/71574-MS

[35] T. Von Schroeter, F. Hollaender, A.C. Gringarten, SPE-77688 presented in the SPE Annual Technical Conference and Exhibition, Sept 29 – Oct 2.(2002) San Antonio, USA. https://doi.org/10.2118/77688-MS

[36] T. Von Schroeter, F. Hollaender, A.C. Gringarten, SPE J. (2004), https://doi.org/10.2118/77688-PA.

[37] M. Levitan, SPE paper # 84290 presented in SPE Annual Technical Conference and Exhibition, 5-8 October (2005), Denver, Colorado. https://doi.org/10.2118/84290-MS

[38] M. Levitan, G.E. Crawfor, A. Hardwick, SPE J. 11 (1), SPE-90680 PA (2006) 35–47, https://doi.org/10.2118/90680-PA.

[39] M. Onur, M. Cinar, D. Ilk, P.P. Valko, T.A. Blasingame, P.S. Hegeman, SPE J. 13 (2), SPE-102575-PA (2008) 226–247, https://doi.org/10.2118/102575-PA.

[40] P.W.M. Corbett, S. Geiger-Boschung, L.P. Borges, M. Garayev, J.G. Gonzalez, C. Valdez, SPE-130252-MS presented in SPE EUROPEC/EAGE Annual Conference and Exhibition, 14-17 June (2010), Barcelona, Spain. https://doi.org/10.2118/130252-MS

[41] R.N. Horne, SPE-27972-MS presented in University of Tulsa Centennial Petroleum Engineering Symposium, 29-31 August (1994), Tulsa, Oklahom. https://doi.org/10.2118/27972-MS

[42] A.Y. Guillot, SPE-11220-PA, SPE Formation Evaluation 1 (3) (1986) 217–226, https://doi.org/10.2118/12958-PA.

[43] M. Levitan, SPE-102484, SPE J. 12 (4) (2007) 420–428, https://doi.org/10.2118/102484-PA.

[44] M. Levitan, G.E. Crawford, A. Hardwick, SPE J. 11 (1), SPE-90680 PA, (2006) 35-47, https://doi.org/10.2118/90680-PA

[45] S.J. Stieber, SPE 2961-MS presented in SPE Fall Meeting AIME, 4-7 October (1970), Houston, Texas. doi:10.2118/2961-MS

[46] W. Bertozzi, D.V. Ellis, J.S. Wahl, Geophysics 46 (10) (1981) 1439–1455.

[47] J.T. Dewan, SPWLA-1986-MM presented in SPWLA Twenty-Seventh Annual Logging Symposium, 9-13 June (1986), Houston, Texas.

[48] Schlumberger, 2016, Interactive Petrophysics Version 3.5 User's Manual, Synergy Ltd., Ternan House, North Deeside Road, Banchory, Kincardineshire AB31 5YR, Scotland.

[49] R.S. Buckles, J. Can. Petroleum Technol. 9 (1) (1965) 42–52.

[50] D.K.J. Brandes, J. Farley, Water Environ. Res. 65 (7) (1993) 869–878.

[51] Synergy web site, June 2016, https://ipdownloads.lr-senergy.com

[52] Kappa Company web site, 2016, https://www.kappaeng.com/software .

[53] D. Bourdet, T.M. Whittle, A.A. Douglas, Y.M. Pirard, World Oil, May (1983) 95–106.

[54] H.K. Van Poolien, Oil Gas J. (Sept. 14., 1964) 138.146. 47 (1961).

[55] Model risk VOSE web site, 2016, http://www.vosesoftware.com